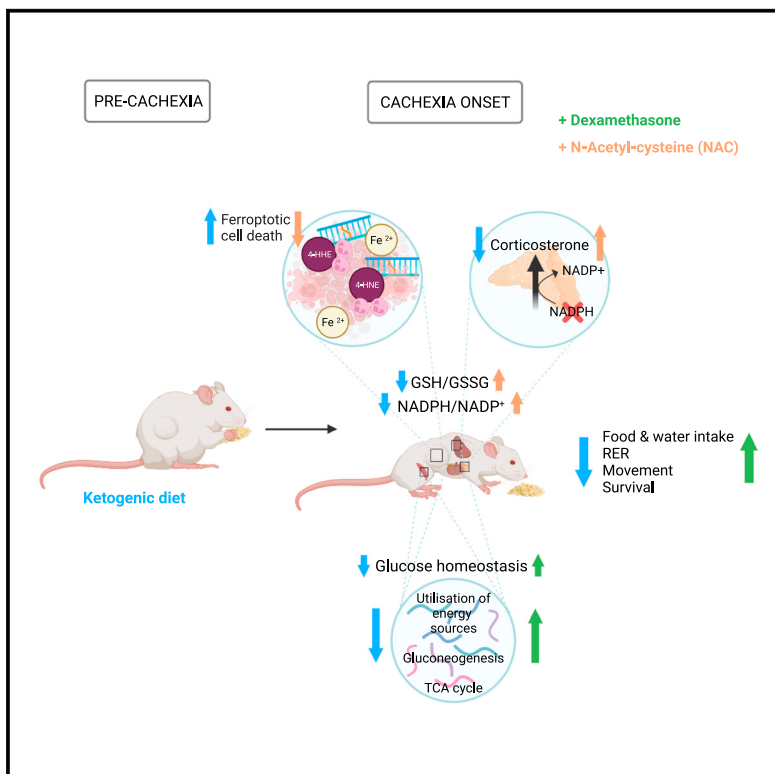


## Ketogenic diet promotes tumor ferroptosis but induces relative corticosterone deficiency that accelerates cachexia

### Graphical abstract



### Authors

Miriam Ferrer, Nicholas Mourikis,  
Emma E. Davidson, ..., Eileen P. White,  
Ashok R. Venkitaraman,  
Tobias Janowitz

### Correspondence

janowitz@cshl.edu

### In brief

Ferrer et al. discover that the anti-cancer effects of a ketogenic diet are uncoupled from survival in mouse models of IL-6-producing cancers. Intratumoral ferroptosis causes a smaller tumor burden, but systemic NADPH depletion induces relative hypocorticosteronemia, which accelerates cachexia onset. These findings highlight the importance of considering both anti-cancer and host effects when investigating the outcome of systemic interventions.

### Highlights

- Ketogenic diet delays tumor growth but accelerates cachexia and shortens survival
- In the tumor, increased lipid peroxidation causes ferroptotic death of cancer cells
- In the host, redox imbalance and NADPH depletion cause corticosterone deficiency
- Dexamethasone plus ketogenic diet delays cachexia and preserves delayed tumor growth





unsaturated lipids through non-enzymatic lipid peroxidation is a recognized source of highly reactive molecules named lipid peroxidation products (LPPs), such as 4-hydroxyhexenal (4-HNE), 4-hydroxyhexenal (4-HHE), and malondialdehyde (MDA), which cause cross-linkage on DNA and proteins through the formation of etheno-adducts.<sup>13,14</sup> Under physiological conditions, lipid peroxidation rates are low and non-toxic because lipid hydroperoxides (LOOHs) are quickly removed from cells by constitutive antioxidants defense systems, such as the NADPH-dependent glutathione (GSH) system.<sup>15,16</sup> When this detoxification fails, the accumulation of LPPs results in a type of programmed cell death dependent on iron that is termed ferroptosis.<sup>17</sup>

Cortisol is the major human glucocorticoid, equivalent to corticosterone in rodents. Cortisol release is part of the physiological response to starvation in cancer cachexia that drives adaptive pathways and regulates nutrient storage, glucose levels, protein breakdown, and lipolysis.<sup>18–20</sup> Biosynthesis of glucocorticoids occurs in the cortex of the adrenal glands through repeated NADPH-dependent enzymatic reduction of cholesterol. This process is under the control of the hypothalamic-pituitary-adrenal (HPA) axis. The inability to mount an adequate stress response due to irreversible damage to the adrenal cortex (e.g., auto-immunity)<sup>21</sup> or pharmacotherapy-induced suppression of the HPA axis<sup>22</sup> presents a life-threatening condition called adrenal insufficiency.

Therefore, glucocorticoid synthesis and the LOOH detoxification pathway share the requirement for NADPH as cofactor, yet their biochemical interdependency has not been explored. This interaction becomes relevant when both pathways simultaneously occur in metabolically stressed organisms (e.g., cachexia) fed a diet with high fat content (e.g., KD).

In this study, we set out to determine the differential effect of KD on tumors and the host organism using two murine models of cancer cachexia. We find that although KD slows tumor growth, it shortens survival by accelerating the onset of cachexia. Mechanistically, increased lipid peroxidation in KD-fed tumor-bearing mice leads to systemic redox imbalance. Within tumors, this results in saturation of the GSH pathway, formation of LPPs, and consequent ferroptotic death of cancer cells. Moreover, we discover that NADPH depletion impairs corticosterone biosynthesis in the adrenal cortex, inducing a relative adrenal insufficiency and metabolic maladaptation in mice fed KD. Treatment with the synthetic corticosteroid dexamethasone delays the onset of cancer cachexia and extends survival of tumor-bearing mice fed KD by improving food intake, metabolic homeostasis, and utilization of nutritional substrates while preserving the anti-tumor response.

The uncoupling of tumor growth from overall survival (OS) illustrates why clinical trials should monitor the host response to nutritional interventions such as KD closely.

## RESULTS

### KD delays tumor growth but shortens OS in two mouse models of cancer cachexia

To investigate the effect of KD on established IL-6-secreting cachexia-inducing cancers and the tumor-bearing host, BALB/c mice bearing subcutaneous C26 colorectal tumors for 14 days and KPC mice (*Kras*<sup>G12D/+</sup>, *Trp53*<sup>R172H/+</sup>, *Pdx-1-Cre*), a genetically

engineered mouse model (GEMM) of pancreatic cancer, with >3–5 mm size tumors were challenged with a low-carbohydrate, moderate-protein, high-fat KD or maintained on normal diet feeding (NF) (Figure S1A; Table S1). Tumor growth was significantly decelerated in mice fed KD in both models, indicating a diet-mediated anti-tumor effect (Figures 1A and 1B). However, KD prompted an earlier onset of cancer cachexia (>15% body-weight loss), thus shortening OS in both C26 and KPC mice fed KD compared with their counterparts fed NF (median OS: 10 days C26/KD, 14 days C26/NF, 6.5 days KPC/KD, 17 days KPC/NF) (Figures 1C, 1D, S1B, and S1C). At endpoint, tumor-bearing mice exhibited loss of subcutaneous and gonadal fat tissue, depletion of quadriceps muscle mass, and splenomegaly, all of which are recognized signs of cachexia (Figures S1D and S1E).

Longitudinal monitoring of blood glucose levels showed an acute decrease in the glucose of littermate (LM) controls and PC controls after introduction of KD that completely recovered after 24 h to similar levels of controls fed NF. By contrast, C26 and KPC tumor-bearing mice on KD did not adapt to the new nutritional source, and their glucose levels kept declining over time, reaching the lowest levels at the cachectic endpoint. Tumor-bearing mice on NF had lower glucose levels than their non-tumor-bearing counterparts but higher than tumor-bearing mice on KD, and they were able to maintain stable glucose measurements until the onset of cachexia when the levels dropped abruptly (Figures 1E and 1F). Circulating ketones were significantly increased in all KD-fed compared with NF-fed groups, but tumor-bearing mice had lower levels compared with their non-tumor-bearing control counterparts on the same diet (Figures 1G and 1H). LM mice on KD had a 2-fold upregulation of hepatic mRNA levels of PPARα target genes that regulate ketogenesis, *Acadm* and *Hmgsc2*, compared with LMs on NF. The expression was also 2-fold higher than in C26 tumor-bearers on KD, which were unable to upregulate the transcriptional targets responsible for ketogenesis, despite the increased dietary substrate. C26 tumor-bearing mice on NF exhibited suppressed transcriptional regulation of ketogenesis compared with NF-fed LMs, as previously described<sup>9</sup> (Figures S1F and S1G). Food intake was decreased in both tumor-bearing groups as cachexia developed (Figures S1H and S1I). Taken together, these data demonstrate that KD impairs the metabolic responses that maintain glucose levels in the tumor-bearing host and does not overcome the maladaptive, tumor-mediated suppression of ketogenesis.

### KD induces formation of etheno-adducts and ferroptotic cell death of cancer cells that can be prevented by NAC

A lipid-enriched diet, such as KD, provides an increased amount of substrate for lipid peroxidation and formation of lipid radicals, which may influence the redox state in the tumor and of the organism. To study the redox state of both the tumor and the host in the context of KD (Table S1), we performed an in-depth metabolomics analysis on liver and tumor tissue of tumor-bearing C26 and LM mice fed KD or NF, in the knowledge that NADPH-dependent detoxification of LOOHs and formation of LPPs may occur. 4-HNE, the major LPP resulting from oxidation of fatty acids, accumulated in the liver of tumor-bearing C26 mice that were fed KD compared with NF-fed tumor-bearing mice. LM on KD had unchanged levels of 4-HNE in the liver compared with

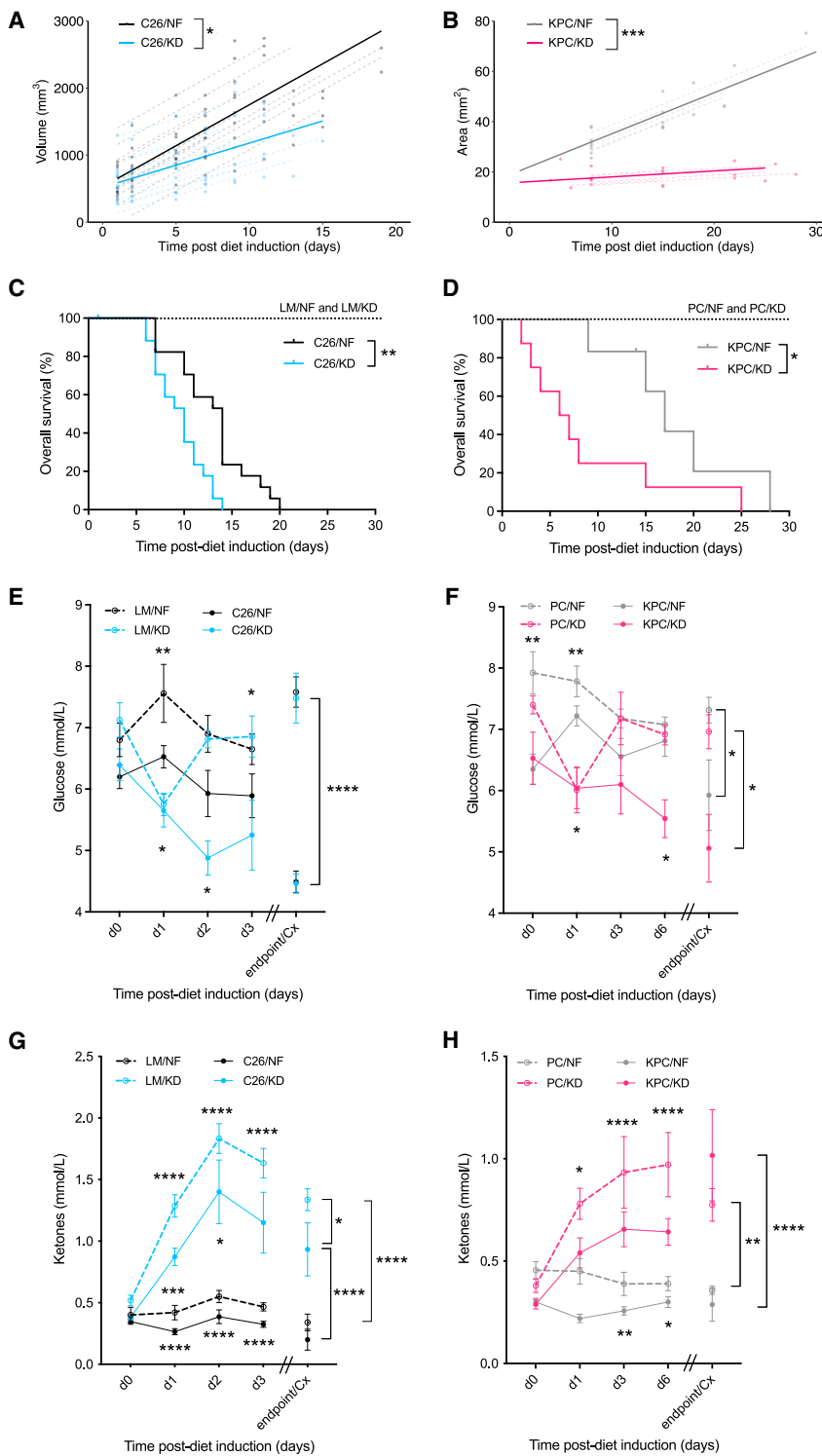


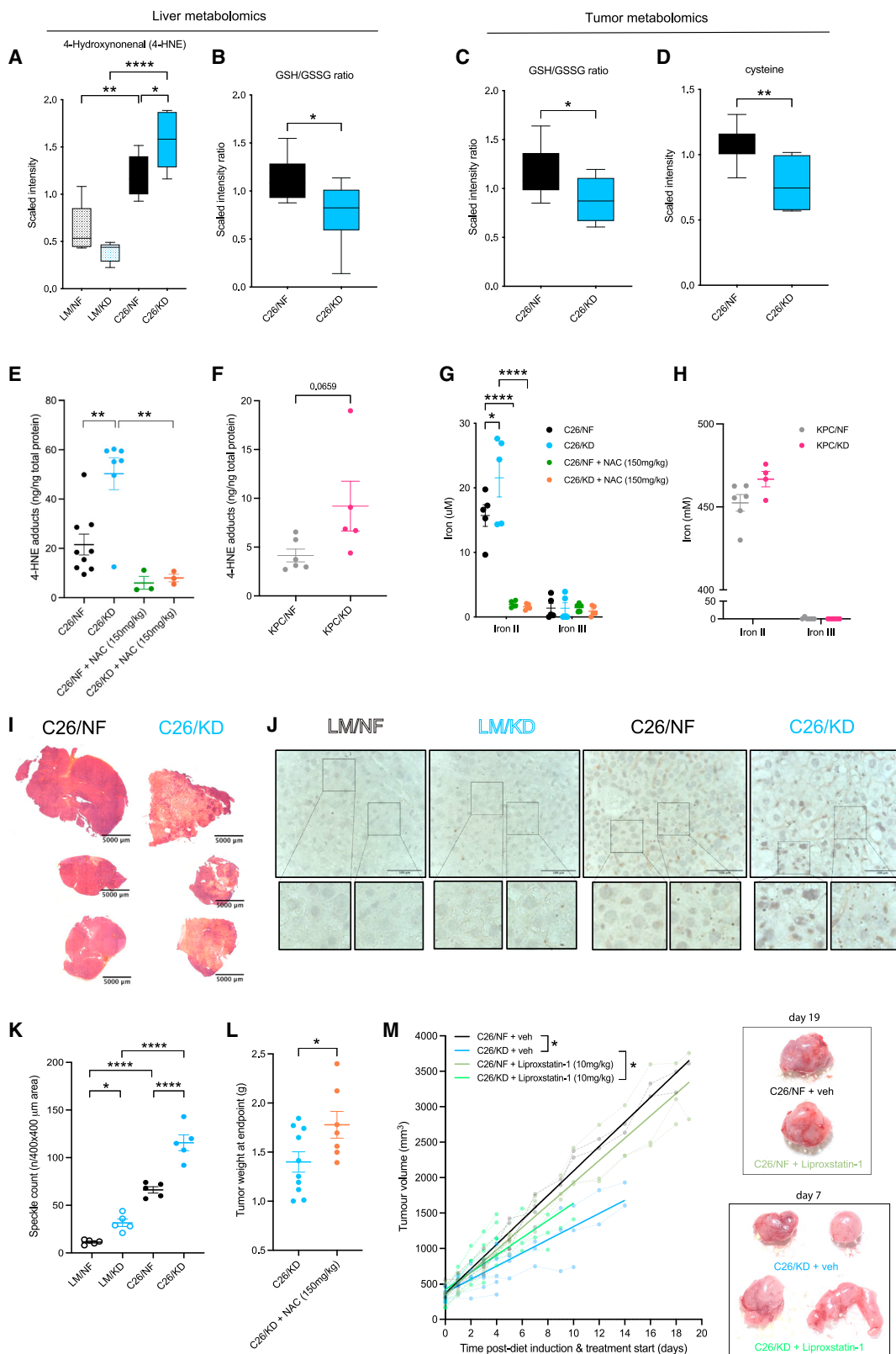
**Figure 1. KD delays tumor growth but shortens OS in C26 and KPC murine models of cancer cachexia**

(A) Longitudinal tumor volume in C26 mice fed KD or NF (n = 12).  
(B) Longitudinal tumor area in KPC mice fed KD or NF (n = 8).  
(C) OS of C26 and LM mice on KD or NF (n = 7 LM, n = 17 C26).  
(D) OS of KPC and PC mice fed KD or NF (n = 5–8).  
(E) and (F) Longitudinal glucose measurements in C26 and LM mice (n = 7–14 LM, n = 20 C26) (E) and in KPC and PC mice (n = 8–10) (F) fed either KD or NF.  
(G) and (H) Longitudinal ketone measurements in C26 and LM mice (n = 5–14 LM, n = 22–23 C26) (G) and in KPC and PC mice (n = 8–10) (H) fed either KD or NF. Overall survival (OS): time until mice reach >15% bodyweight loss. Differences in (A) and (B) were assessed by fitting a mixed-effect model with a random component for each individual mouse. Tumor growth was followed to cachexia or tumor size endpoint for all groups. Kaplan-Meier curves in (C) and (D) were statistically analyzed by using the log-rank (Mantel-Cox) test. Two-way ANOVA statistical tests with Tukey's correction for post hoc comparisons were performed in (E)–(H). \*p < 0.05; \*\*p < 0.01; \*\*\*p < 0.001; \*\*\*\*p < 0.0001.

NF-fed LM, suggesting that its production was efficiently detoxified (Figures 2A and S2A). GSH to GSSG ratio in liver and tumor of C26 tumor-bearing mice on KD was decreased compared with those on NF, suggesting an ongoing utilization of the reductive power of GSH molecules with the purpose of detoxifying LOOHs (Figures 2B and 2C). Tumor metabolomics of C26 mice

fed KD or NF were separated by PCA (Figure S2B). The rate-limiting precursor metabolite for GSH biosynthesis, cysteine, was also decreased in tumors from C26 mice fed KD (Figure 2D), whereas ophthalmate, a biomarker for oxidative stress and GSH depletion,<sup>23</sup> significantly accumulated in KD tumors (Figure S2C). Other indicators of redox perturbation, such as the collapse of the antioxidant carnosine<sup>24</sup> (Figure S2D) and evidence of hypotaurine to taurine oxidation (Figures S2E and S2F),<sup>25</sup> were present in tumors from C26 KD-fed mice. These data are compatible with an increased formation of toxic and highly mutagenic LPPs due to saturation of the GSH pathway in tumors from C26 mice on KD compared with those fed NF. Adduct formation by the LPP 4-HNE was significantly elevated in the tumors from C26 and KPC mice fed KD compared with those fed NF (Figures 2E and 2F). 4-HNE adducts in KD-fed C26 mice were prevented with the administration of N-acetyl cysteine (NAC), an antioxidant that boosts GSH biosynthesis, prevents LOOH peroxidation, and therefore prevents the formation of LPPs (Figures 2E, S2A, and S2G).

Accumulation of LPPs results in ferroptosis,<sup>26</sup> an iron-dependent cell death that has previously been described in cysteine-depleted tumors.<sup>27</sup> To explore the possibility that ferroptotic cell death in tumors from KD-fed mice is partly responsible for

**Figure 2. KD induces ferroptotic cell death of cancer cells that can be prevented by NAC**

(A and B) Quantification by UPLC-MS/MS of 4-HNE (A) and GSH/GSSG ratio (B) in the liver of C26 and LM mice on KD or NF ( $n = 5-8$ ). (C and D) Quantification by UPLC-MS/MS of GSH/GSSG ratio (C) and cysteine (D) in the tumor of C26 mice ( $n = 7$ ).

(legend continued on next page)



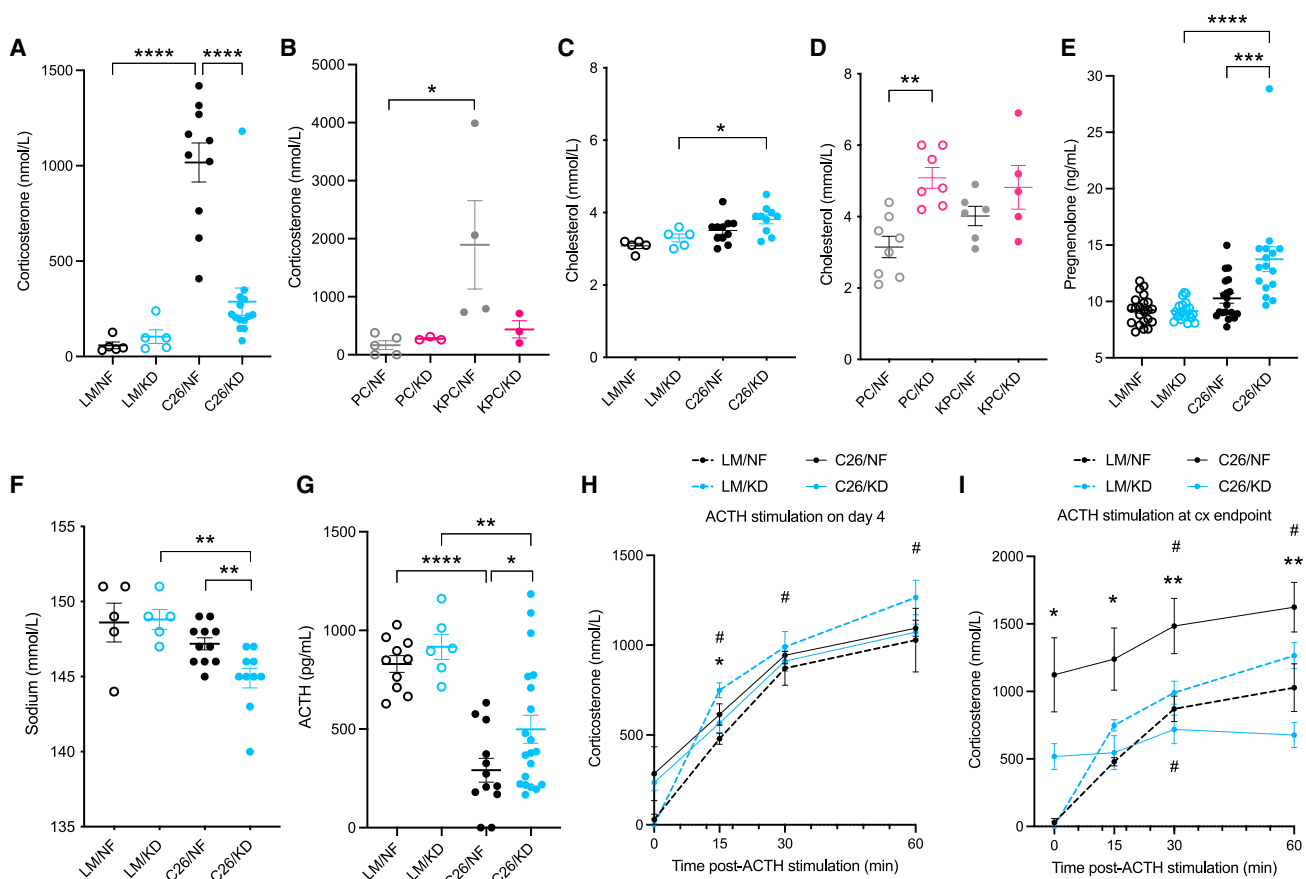


**Figure 3. KD induces relative corticosterone deficiency in C26-tumor-bearing mice**

(A and B) Plasma corticosterone levels in cachectic C26 and LM mice ( $n = 5$  LM,  $n = 10\text{--}14$  C26) (A) and cachectic KPC and PC mice ( $n = 3\text{--}5$ ) (B) fed KD or NF. (C and D) Plasma cholesterol levels in cachectic C26 and LM mice ( $n = 5$  LM,  $n = 10\text{--}11$  C26) (C) and in cachectic KPC and PC mice ( $n = 5\text{--}8$ ) (D) fed KD or NF. (E-G) Pregnenolone (n = 16–22) (E), sodium (n = 5 LM, n = 10–11 C26) (F), and ACTH (n = 6–10 LM, n = 12–20 C26) (G) levels in plasma of cachectic C26 and LM mice on KD or NF.

(H and I) Synacthen test in C26 and LM mice 4 days after diet change (n = 4–5) (H) and in cachectic C26 and LM mice at endpoint (n = 5–8) (I). One-way ANOVA with Tukey's correction for post hoc testing was used in (A)–(G). Two-way ANOVA statistical tests with Tukey's correction for post hoc comparisons were performed in (H) and (I). # $p < 0.05$  compared with time = 0. \* $p < 0.05$ ; \*\* $p < 0.01$ ; \*\*\* $p < 0.001$ ; \*\*\*\* $p < 0.0001$ .

glands of tumor-bearing mice fed KD compared with those fed NF. One of the major actions of aldosterone, a mineralocorticoid hormone derived from downstream processing of corticosterone, is sodium retention. We noted a relative hyponatremia in C26 tumor-bearing mice fed KD compared with those fed NF and LM on either diet (Figure 3F), which may, at least in part, be a result of diminished, adrenally derived mineralocorticoid action. This further supports an impaired hormone biosynthesis in the adrenal glands of these mice.

The adrenal glands are part of the HPA axis. The adrenocorticotrophic hormone (ACTH) is a hormone produced by the pituitary gland that drives corticosterone production in the adrenal glands. Elevated circulating corticosterone levels induce negative feedback on the HPA axis and inhibit ACTH release. In order to assess whether the impaired synthesis of corticosterone in tumor-bearing mice fed KD is (1) a localized phenomenon in the cortex of the adrenal glands; (2) due to an upstream defect in the HPA axis, such as inadequate ACTH production by the pituitary gland; or (3) a combination

of both, we quantified ACTH in the plasma of C26 mice and LM-fed NF or KD. At endpoint, levels of ACTH detected in cachectic tumor-bearing mice were more broadly distributed compared with levels seen in non-tumor-bearing control mice, and there was a small but significant increase in ACTH in C26 KD-fed mice compared with those NF-fed, suggestive again that the primary issue pertaining to this relative corticosterone deficiency was sited within the adrenal glands (Figure 3G). However, given the variance in ACTH levels, a minor contribution from upstream mechanisms to the observed hypocorticosteronemia cannot be excluded.

Because corticosterone release can potentially be driven by direct stimulation of the adrenal glands by non-ACTH peptides, such as IL-6,<sup>35–37</sup> and the C26 model is known to display high IL-6 levels,<sup>9</sup> we quantified circulating levels of this cytokine. No diet-mediated differences between the tumor-bearing groups were observed (Figure S3D), indicating that IL-6 does not contribute to the relative corticosterone deficiency observed in KD-fed tumor-bearing mice.

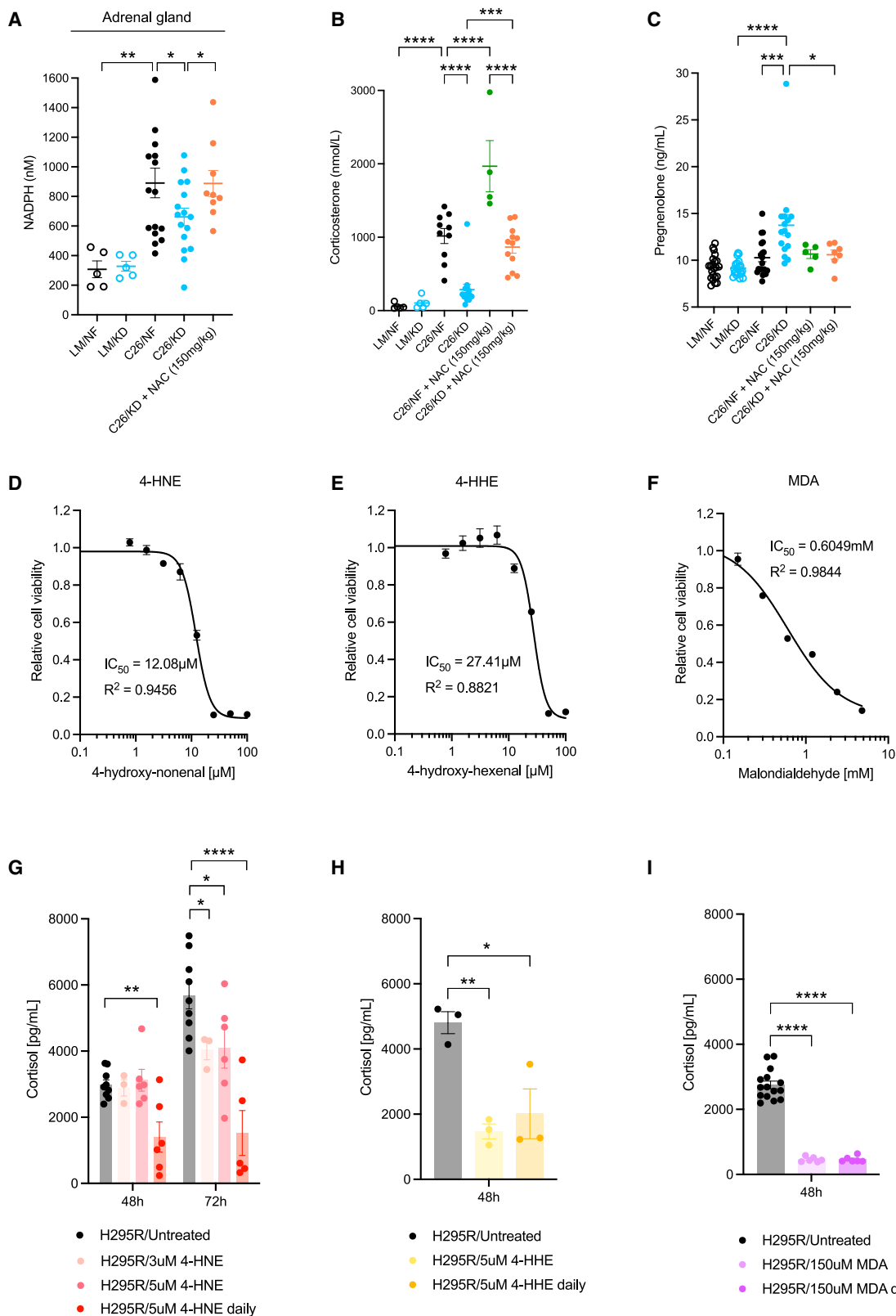


**Figure 4. NAC rescues adrenal function *in vivo* and LPPs suppress cortisol production *in vitro***

(A) NADPH quantification in the adrenal glands of C26 and LM mice fed KD or NF, and C26 mice fed KD treated with NAC (n = 5 LM, n = 9–16 C26). (B and C) Corticosterone (n = 5–14) (B) and pregnenolone (n = 5–21) (C) levels in plasma of C26 and LM mice fed KD or NF, untreated or treated with NAC.

(legend continued on next page)

To assess adrenal gland responsiveness, we undertook ACTH stimulation tests using synthetic ACTH (synacthen test) at two time points: the first cohort was studied 4 days after diet change (day 18 post-C26 injection), and a second cohort was studied at the onset of cachexia. On day 4 after diet switch, both tumor-bearing C26 groups had higher baseline corticosterone levels compared with LM. In response to ACTH administration, tumor-bearing C26 mice on NF had a stronger response to ACTH than their LM on NF. Conversely, corticosterone upregulation in tumor-bearing C26 mice on KD was significantly reduced compared with the response of LM on KD (Figure 3H). Thus, our results show signs of malfunction of the stress axis in tumor-bearing mice fed KD even at this early stage. At cachexia endpoint, baseline corticosterone levels pre-stimulation were significantly elevated in tumor-bearing C26 mice on NF compared with those on KD (Figure 3I). Upon ACTH injection, plasma corticosterone increased over time in tumor-bearing C26 mice fed NF and in LM, whereas levels in tumor-bearing C26 mice fed KD did not change significantly. After 60 min, levels of corticosterone in tumor-bearing C26 mice fed NF were almost 2.5-fold higher than in those fed KD. Both LM groups showed similar responses and reached peak levels comparable to those of tumor-bearing C26 mice on NF at baseline (Figure 3I). These data point toward an intrinsic difficulty in the adrenal glands of KD-fed tumor-bearing mice to respond to hormonal stimulation and release corticosterone compared with NF-fed tumor-bearing mice. Together, we provide evidence that KD drives the development of a relative adrenal insufficiency in tumor-bearing mice.

#### NAC treatment rescues corticosterone synthesis in tumor-bearing mice fed KD

In order to identify the mechanism underlying the relative deficiency in corticosterone biosynthesis in tumor-bearing mice fed KD, we next explored the interaction of the GSH pathway (Figure S2A) and the corticosterone synthesis pathway (Figure S3A) through their common need of NADPH sources. Targeted quantification of NADPH and NADPH/NADP<sup>+</sup> ratio in the adrenal glands of cachectic mice and controls showed higher levels of NADPH in tumor-bearing C26 mice fed NF compared with LM-fed NF because it would be anticipated in the context of an ongoing release of corticosterone. However, NADPH levels and the NADPH/NADP<sup>+</sup> ratio were diminished in the adrenal glands of C26 mice fed KD compared with C26 mice fed NF. Administration of NAC, a cysteine prodrug that replenishes intracellular GSH levels in the absence of NADPH consumption, rescued NADPH levels and the NADPH/NADP<sup>+</sup> ratio in these mice (Figures 4A and S3E). Of note, NADP(H) are challenging targets for quantitative analysis due to their transient nature and chemical instability during sample extraction and processing, which is reflected in the variance of measurements within groups. Nevertheless, taken together, these data indicate that the increased demand for NADPH in the process of detoxification of LOOHs leads to a shortage of this cofactor, which then is not available for use in the synthesis of corticosterone and

leads to low levels of this stress hormone in tumor-bearing mice fed KD.

To examine this hypothesis further, we measured corticosterone levels in tumor-bearing mice fed KD or NF and treated with NAC. Circulating corticosterone was markedly higher in the NAC-treated groups compared with untreated and control groups on the same diet (Figure 4B). Simultaneously, pregnenolone accumulation in KD-fed tumor-bearing mice was no longer detected upon NAC treatment (Figure 4C), indicating conversion of this early intermediate to downstream intermediates of corticosterone biosynthesis and ultimately to corticosterone. Therefore, promoting GSH production through NAC diminishes the need of NADPH oxidation, consequently increasing GSH's LOOH-detoxifying activity and preventing NADPH depletion. NADPH availability enables an appropriate synthesis of corticosterone in the adrenals and leads to the physiological rise in systemic corticosterone levels in the context of metabolic stress associated with cachexia.

#### LPPs exposure decreases cortisol production in a human adrenal cortex-derived cell line

After their production, LPPs react with intracellular proteins and DNA. They are enzymatically reduced via phase I (ALDH, AOR, AKR, and CYPs) and phase II (GSH) metabolism, and these reductive reactions are NADPH dependent.<sup>38</sup> We next implemented the human adrenal cortex-derived cell line, H295R, to test the direct effects of LPPs on cortisol synthesis *in vitro*. We first identified doses of 4-HNE, 4-HHE, and MDA that did not affect viability of H295R cells upon exposure (Figures 4D–4F). Single or daily treatment of H295R cells with tolerated doses of 4-HNE, 4-HHE, or MDA led to lower cortisol production after 48 and 72 h compared with the cortisol levels released to the media by untreated adrenocortical cells (Figures 4G–4I). Thus, these data suggest that LPPs can directly suppress cortisol production in adrenocortical human cells, most likely due to an NADPH-depleting effect, similar to the one observed *in vivo*.

#### GDF-15 is elevated in cachexia and increased by KD

Although the KD-mediated biochemical impairment of the adrenal glands stress response and resulting defective glucocorticoid biosynthesis in tumor-bearing mice described above can account for shortened survival, it does not necessarily explain reduction in food intake. GDF-15, a transforming growth factor (TGF)- $\beta$  superfamily member that is produced by cells under stress, mediates reduced food intake by binding its cognate receptor GFRAL in the area postrema.<sup>39</sup> It has been implicated in the anorectic response in cancer cachexia<sup>40</sup> and in aldehyde toxicity-induced anorexia.<sup>41</sup> In keeping with these findings, we observed elevated circulating GDF-15 levels in cachectic NF-fed C26 mice, which were further elevated in cachectic KD-fed mice (Figure 5A), reflecting the systemic oxidative and metabolic stress of the organism and explaining at least in part the reduced food intake observed in the cachectic phase of the disease (Figures S1F and S1G).

(D–F) Viability of H295R cells treated with 4-HNE (D), 4-HHE (E), or MDA (F) ( $n = 3$  independent experiments) relative to vehicle-treated control cells.

(G–I) Cortisol levels upon exposure of H295R cells to 4-HNE ( $n = 3\text{--}6$ ) (G), 4-HHE ( $n = 3\text{--}6$ ) (H), and MDA ( $n = 6\text{--}15$ ) (I).

One-way ANOVA with Tukey's correction for post hoc testing was used in (A)–(C) and (G)–(I). \* $p < 0.05$ ; \*\* $p < 0.01$ ; \*\*\* $p < 0.001$ ; \*\*\*\* $p < 0.0001$ .

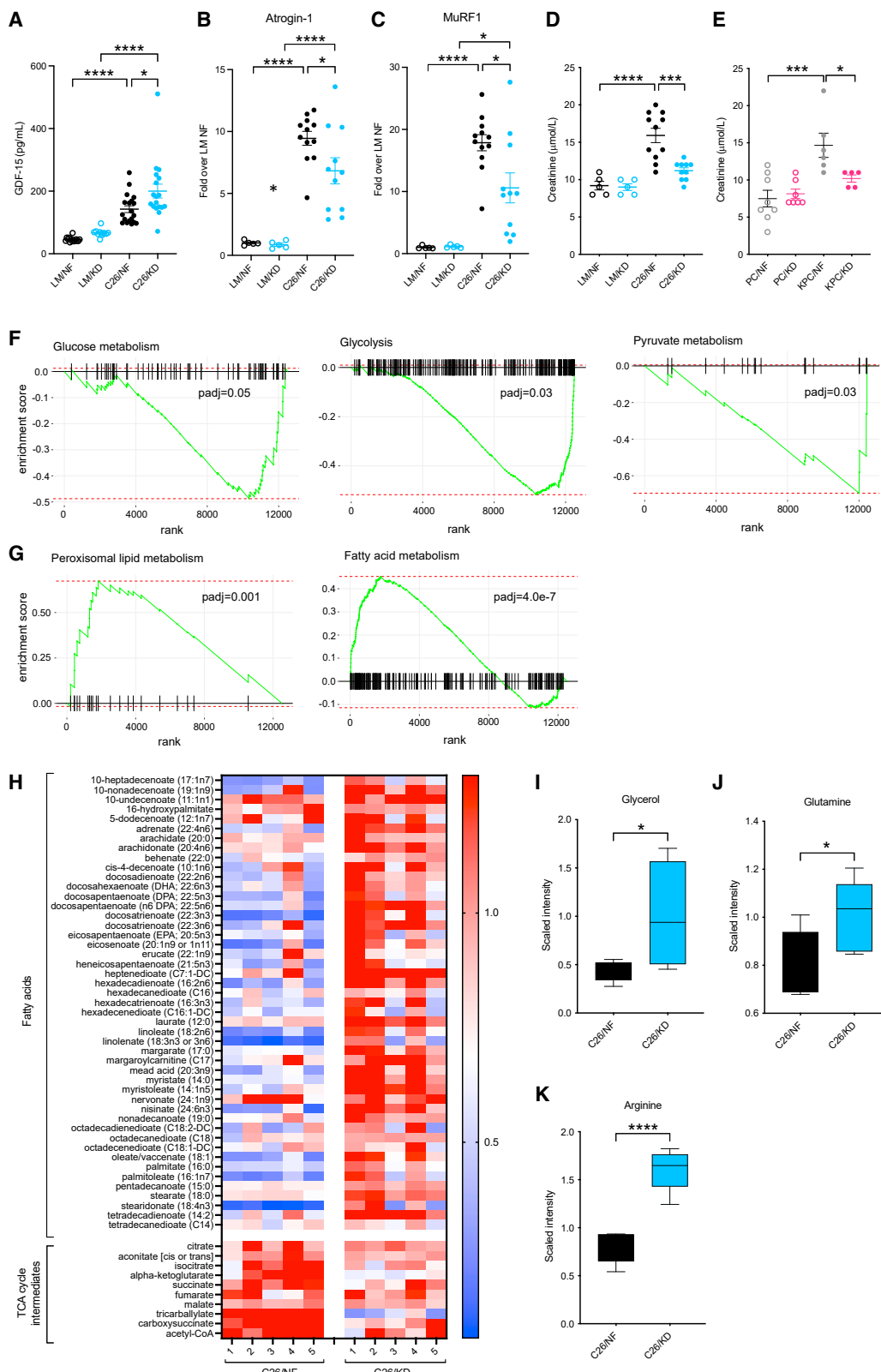


**Figure 5. Metabolic adaptation in the context of cachexia is impaired in KD-fed tumor-bearing mice**

(A) Plasma levels of GDF-15 in C26 and LM mice fed KD or NF (n = 11–19).

(B and C) mRNA levels of the E3 ligases Atrogin-1 (B) and MuRF1 (C) in the quadriceps of C26 and LM mice fed KD or NF (n = 5 LM, n = 12 C26).

(legend continued on next page)



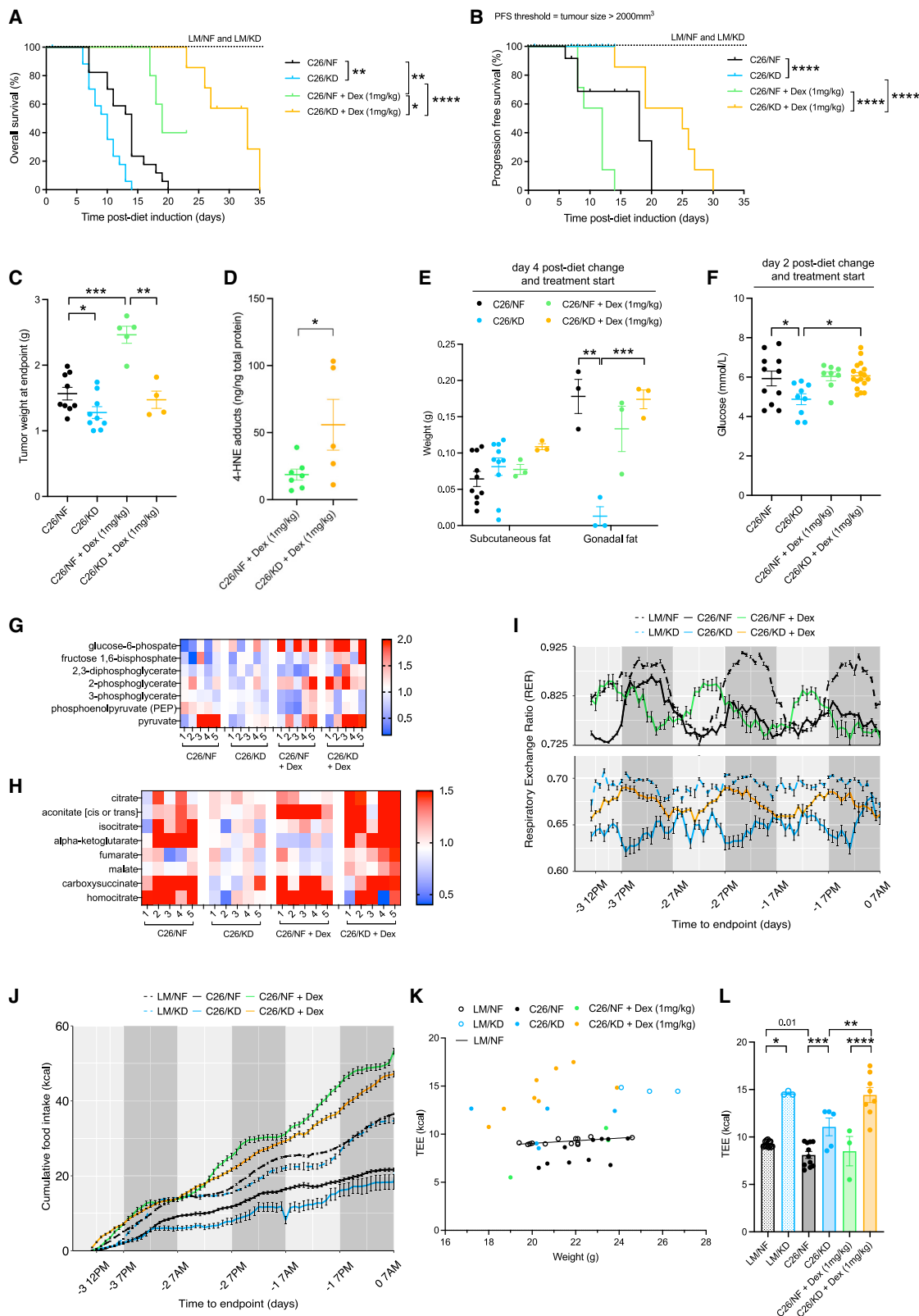


**Figure 6. Dexamethasone treatment extends survival and improves metabolic adaptation of C26 mice fed KD**

(A and B) OS (A) and PFS (B) of C26 mice fed KD or NF, untreated or treated with dexamethasone, and LM mice fed with either diet ( $n = 7$  LM,  $n = 17-18$  C26,  $n = 7$  C26 + Dex).



causes poor prognosis and early death of patients with cancer,<sup>51</sup> suggesting that therapeutic support of host metabolic adaptation may extend lifespan. Indeed, we find that rescue of the systemic metabolic adaptation (KD + Dex) suppresses cancer cachexia and extends survival without altering tumor burden, indicating that it is the systemic metabolic imbalance that is most lethal. Moreover, targeting metabolic dependency of cancer cells shows therapeutic promise in stalling or delaying tumor growth. However, our results show that careful consideration of this paradigm is indicated if a chosen nutritional intervention challenges both the metabolism of the organism and the tumor. This is specifically the case for KDs, which are currently tested in clinical trials. Here, the anti-cancer effect may be offset by the inability of the organism to utilize the lipid nutrients because the reprogramming of systemic metabolism, muscle and fat loss, and reduced food intake are hallmarks of cancer progression and cachexia.<sup>52</sup>

Glucocorticoids, and specifically cortisol, regulate metabolism in conditions of stress. Dexamethasone is a corticosteroid commonly used as supportive care for patients with cancer undergoing standard care in order to lower the immune response, reduce inflammation, and prevent or treat cancer-related conditions, such as anemia, cerebral oedema, hypersensitivity, hypercalcemia, and thrombocytopenia. Side effects of dexamethasone treatment include weight gain, increased glucose levels, and fat accumulation. However, our study shows that what would normally be considered in the clinic as metabolic aftereffects of dexamethasone may become beneficial for pre-cachectic organisms on a fat-rich diet that exhibits metabolic imbalance and inadequate response to preserve glucose levels (e.g., HPA axis unresponsiveness).

Moreover, some preclinical studies and clinical trials suggest that corticosteroid-induced immunosuppression might dampen the activity of cancer chemo-immunotherapy and increase risk of cancer recurrence,<sup>53–55</sup> but this is contradicted by others.<sup>56,57</sup> This ongoing debate on the potential impact of corticosteroids on the anti-tumor immune response is illustrated in our preclinical work, as we observe that dexamethasone administration reduces PFS in NF-fed mice, whereas tumor growth in KD-fed mice is unaffected by dexamethasone. Thus, the patients' dietary intake and nutritional state may be confounding factors in clinical trials that investigate the immunosuppressive impact of corticosteroids co-treatment in cancer. Nutritional interventions combined with the minimum effective dose of corticosteroids should be preferred.

Dietary interventions can be used to enhance anti-cancer therapy and improve clinical outcomes.<sup>58–60</sup> Cancer cells exhibit high dependency on glucose,<sup>1</sup> which can be exploited by specific diet regimens. Diets can also have an effect on the immune system and influence the anti-tumor response. KDs have been previously studied in patients with cancer and shown to be safe, feasible, and even to have anti-cancer effects. These low-carbohydrate diets reduce circulating glucose levels and suppress pro-tumorigenic mitogens, which combine to limit tumor nutrient uptake. In this study, we show evidence that supports that KD may be slowing down tumor growth not only via nutrient deprivation but also through an ongoing accumulation of LPPs that induces ferroptotic cell death within the tumor. The amino acid composition of the KD (extended data

Table S1) may also be contributing to the observed phenotype because the 9-fold decrease in cystine intake can induce ferroptosis independently of fatty acids,<sup>27</sup> and the changes in metabolism and energy expenditure of KD-fed mice could be partially attributed to a decrease in methionine intake.<sup>61</sup>

We note that the effect of KD on the host is likely context-dependent: it is detrimental for both the tumor and the host that has been metabolically reprogrammed by the established tumor, but KD has no impact on non-tumor-bearing organisms that are able to adapt their metabolism to the nutritional intake. Even if they grow a tumor later on while on KD, the tumor-induced metabolic reprogramming is delayed due to its decelerated growth. This explains differential results in the literature<sup>62</sup> and evidences the importance of dosing and timing in the clinic.

Without independent validation of our results, it is perhaps too early to suggest that KD and glucocorticoid co-administration may be a therapeutic strategy for patients with IL-6-elevating cancers. Translational studies may find that the relative adrenal insufficiency may only be subclinical in humans because our pre-clinical study shows lack of an appropriate upregulation of cortisol in the context of metabolic stress, not a complete absence of the hormone. Thus, HPA axis activity should be assessed in patients with a lipid-rich nutritional intake because this may have effects in systemic metabolism and therapeutic outcome, even in asymptomatic patients.

Nevertheless, the reduced tumor growth and prolonged survival of dexamethasone-treated KD-fed mice compared with NF-fed mice with or without dexamethasone is an encouraging finding. A limitation to this concept is a lack of the exact understanding of how glucocorticoids rescue metabolism in the context of a reprogrammed organism challenged with KD. Although this may limit the ability for longitudinal monitoring of the molecular response in patients on the combination intervention, weight trajectories and glucose levels may be suitable and readily obtainable biomarkers for clinical studies.

### Conclusions

Our study highlights that the outcome of systemic interventions cannot necessarily be extrapolated from the effect on the tumor alone, but that they have to be investigated for anti-cancer and host effects. In model systems with established tumors that elevate IL-6, the opposing effect of KD on delayed tumor growth and induction of cachexia leads to a dominant-negative effect on survival. These findings may be relevant to clinical research efforts that investigate the potential benefit of KD for patients with cancer.

### Limitations of the study

This study implemented model systems of colorectal and pancreatic cancer that are known to recapitulate clinical disease progression from early cancer to cachexia, but clinical validation of our work is needed. We acknowledge that not all cancers lead to IL-6 elevations and therefore cannot comment on the transferability of our findings to other cancers. The use of male mice only is another limitation of this study, and an equivalent study is required in order to assess potential differences and similarities of the effects of KD in females. The time course of disease progression and metabolic reprogramming in patients with cachexia-inducing tumors has not yet been resolved. We here



















**Western blotting**

Cells were lysed in RIPA buffer (50mM Tris HCl, pH 7.4, 150mM NaCl, 0.5% deoxycholate, 0.1% sodium dodecyl sulphate, 1% NP-40) (#89901; Thermo Fisher) containing protease inhibitors (#78442; Thermo Fisher) and 1 mM dithiothreitol (DTT) (#A39255; Thermo Fisher). Whole cell extracts were separated by electrophoresis, transferred onto nitrocellulose membranes (#88025; Thermo Fisher) and blocked in 5% non-fat dry milk (#1706404; Bio-Rad) dissolved in 0.1% Tween/TBS. Membranes were incubated with primary antibodies: BAX Rabbit mAb (#50599-2-Ig; Proteintech, 1:500),  $\beta$ -Actin Rabbit mAb (#4967; Cell Signaling Technology, 1:5000) and Caspase-3 (D3R6Y) Rabbit mAb (#14220; Cell Signaling, 1:1000), overnight at 4°C followed by washing in 0.1% Tween/TBS. Membranes were incubated with Goat Anti-Rabbit IgG H&L (HRP) secondary antibodies (#ab205718; Abcam, 1:5000) at 25°C for 1h and washed thrice prior to signal detection. Membranes were developed by exposure in a dark room through chemiluminescence using ECL reagent (#32106; Thermo Fisher).

**qRT-PCR**

mRNA was extracted from frozen tissues using QIAzol Lysis Reagent (#79306; Qiagen) and the Tissue Lyser II (#85300; Qiagen), following the manufacturer's protocol for the RNeasy Lipid Tissue Mini Kit (#74804; Qiagen) in an automated manner with the QIAcube Connect (#9002864; Qiagen). Concentration and purity of aqueous RNA was assessed using a NanoDrop Spectrophotometer (#ND-ONE-W; Thermo Fisher). mRNA templates from muscle and liver samples were diluted to 2ng/ $\mu$ l and mRNA was analyzed by quantitative Real-Time PCR using the TaqMan RNA-to-CT 1-Step Kit (#4392653; Thermo Fisher). mRNA levels were normalized to either Rn18s (liver) or Tbp (quadriceps) using the ddCt method. The following TaqMan primers were used: Mm01277044\_m1 (Tbp); Mm03928990\_g1 (Rn18s); Mm00440939\_m1 (Ppara); Mm01323360\_g1 (Acadm); Mm00550050\_m1 (Hmgcs2); Mm00499523\_m1 (Fbxo32); and Mm01185221\_m1 (Trim63).

**RNA-sequencing**

RNA extracted from frozen tissues via QIAzol Lysis Reagent (#79306; Qiagen) was run through RNeasy spin columns following the RNeasy Lipid Tissue Mini Kit in an automated manner with the QIAcube Connect (#9002864; Qiagen). Integrity was confirmed using RIN values with a cut-off of 8. Libraries were prepared by the Next Gen Sequencing Core at CSHL using the Illumina TruSeq mRNA Stranded Sample prep kit (96 index High Throughput) and normalized using Kapa Biosystem's Library Quantification Kit. NextSeq High Output Paired-End 150bp was run for sequencing.

For the analysis, reads were aligned to the mouse genome version GRCm38.74 and read counts were obtained using “biomaRt” R package. “org.Mm.eg.db” R package was used for genome wide annotation. Read counts were normalized and tested for differential gene expression using the Bioconductor package “edgeR”. Multiple testing correction was applied using the Benjamini-Hochberg procedure (FDR <0.05). “fgsea” and “dplyr” packages were used for GSEA in R. GSEA was performed by ranking all genes tested in RNA-Seq using  $-\log_{10}$  (p-values) derived from differential expression analyses and testing against MSigDB Hallmark gene sets and Canonical pathways KEGG gene sets. Results were curated using a p-adj <0.05 threshold.

**QUANTIFICATION AND STATISTICAL ANALYSIS**

Data were expressed as the mean  $\pm$  SEM unless otherwise stated. Statistical analyses were performed using GraphPad Prism 7.03 software or RStudio software. Normality of data distribution was tested with the Shapiro-Wilk test. The log-rank (Mantel-Cox) test was used to compare survival distributions. Two-tailed Student's t-test were used to compare two groups. When comparing 3 or more groups, one-way ANOVA with Tukey's correction for post-hoc testing was used. For statistical comparison of quantitative data at different times, unpaired two-tailed Student's t-tests were performed at each timepoint with the Holm-Sidak method correction for multiple comparisons. To analyze multiple parameters, such as the main independent effect of diet and cancer and the interaction of both factors, two-way ANOVA tests were used. All cell-based in vitro experiments were independently repeated three times in triplicate. For global metabolic profiling of liver and tumor, a Principal Component Analysis (PCA) was performed. Differences in tumor growth were assessed by fitting a mixed effect model with coefficients for the intercept, slope and the difference in the slope between experimental groups, and a random component for each individual mouse. Significance was assessed by testing whether the coefficient for the difference in the slope was significantly different from zero using a t-test. One-way ANCOVA was conducted to determine statistical significances in on total energy expenditure (TEE) controlling for weight. P-values and sample size can be found in main and supplementary figure legends.

**Supplemental information**

**Ketogenic diet promotes tumor ferroptosis  
but induces relative corticosterone deficiency  
that accelerates cachexia**

Miriam Ferrer, Nicholas Mourikis, Emma E. Davidson, Sam O. Kleeman, Marta Zaccaria, Jill Habel, Rachel Rubino, Qing Gao, Thomas R. Flint, Lisa Young, Claire M. Connell, Michael J. Lukey, Marcus D. Goncalves, Eileen P. White, Ashok R. Venkitaraman, and Tobias Janowitz

## **Supplemental information**

*Ferrer et. al.*

“Ketogenic diet promotes tumor ferroptosis but induces relative corticosterone deficiency that accelerates cachexia”

	Standard diet (PicoLab Rodent Diet 20)	Ketogenic diet (AIN-76A Modified)
Fat (%)	10.6	75.1
Protein (%)	20	8.6
Carbohydrates (%)	52.9	3.2
Fiber (%)	4.7	4.8
Ash (%)	6.1	3
Moisture (%)	<10	<10
Caloric profile (kcal/g)	4.07	7.24
Cystine (g/kg)	2.8	0.3
Methionine (g/kg)	7	2.2

**Supplemental Table 1. Macronutrient composition and caloric profile of standard and ketogenic diets, related to Figure 1.**

**Figure S1**

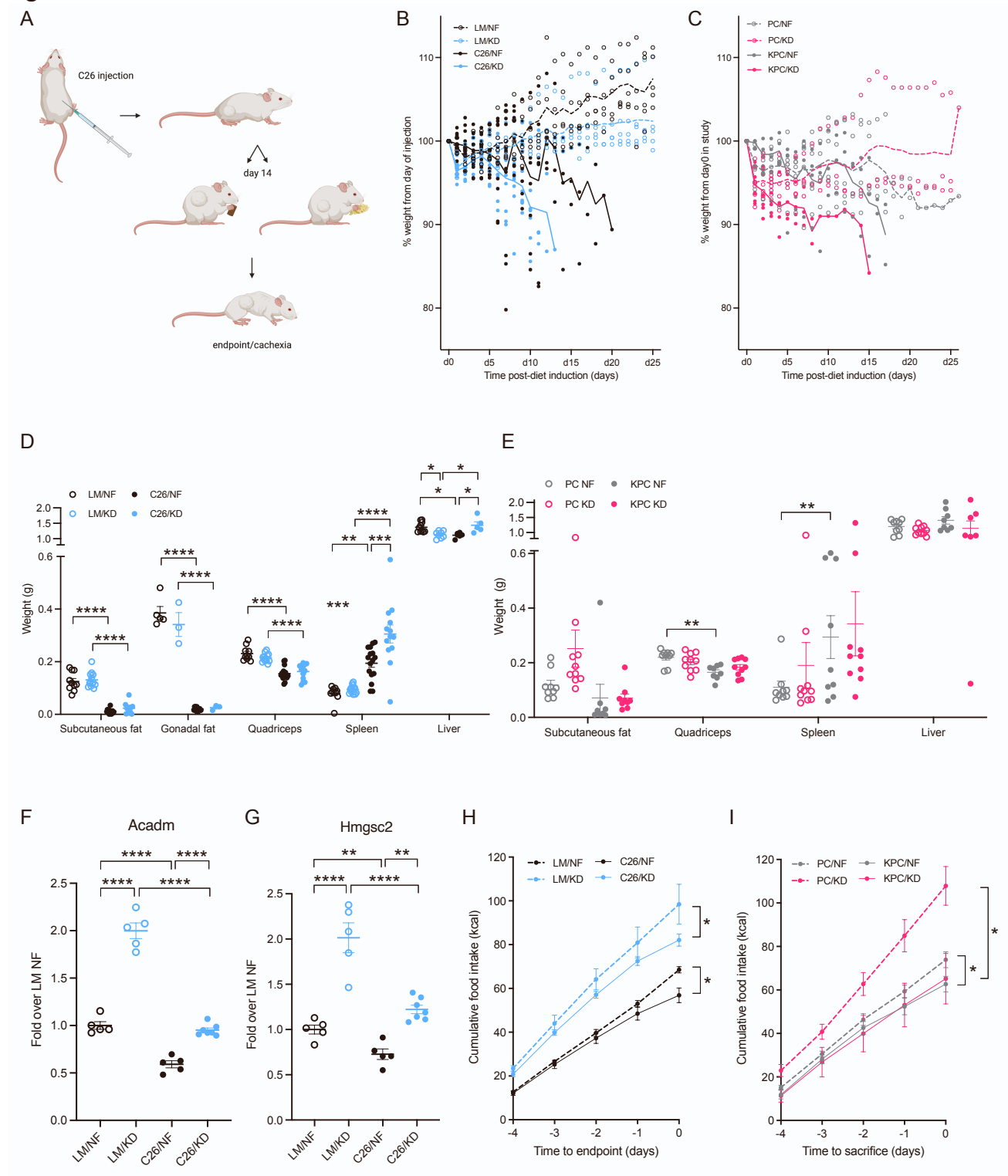


**Figure S1. Cachectic phenotype of C26 and KPC murine models, related to Figure 1.** (A) Graphical summary of the experimental protocol (Created with BioRender.com). (B-C) Weight trajectories of C26 and LM mice (C), and KPC and PC mice (C) on KD or NF diets since they were enrolled into the study until they reached cachectic endpoint. (D-E) Organ weights of cachectic C26 and LM mice ( $n=10-15$ ) (D), and cachectic KPC and PC mice ( $n=9-10$ ) (E) fed either KD or NF diets. (F-G) mRNA expression of the PPAR $\alpha$  target genes Acadm (F) and Hmgsc2 (G) in C26 and LM mice fed KD or NF ( $n=5-7$ ). (H-I) Cumulative food intake of KD- or NF-fed C26 and LM mice ( $n=5$  LM,  $n=7-13$  C26) (H), and KD- or NF-fed KPC and PC mice ( $n=5-6$ ) (I) during the last 4 days before endpoint.

One-way ANOVA with Tukey's correction for post hoc testing was used in (D-G). Two-way ANOVA statistical tests with Tukey's correction for post hoc comparisons were performed in (H-I). \* p-value < 0.05, \*\* p-value < 0.01, \*\*\*\* p-value < 0.0001.

**Figure S2**

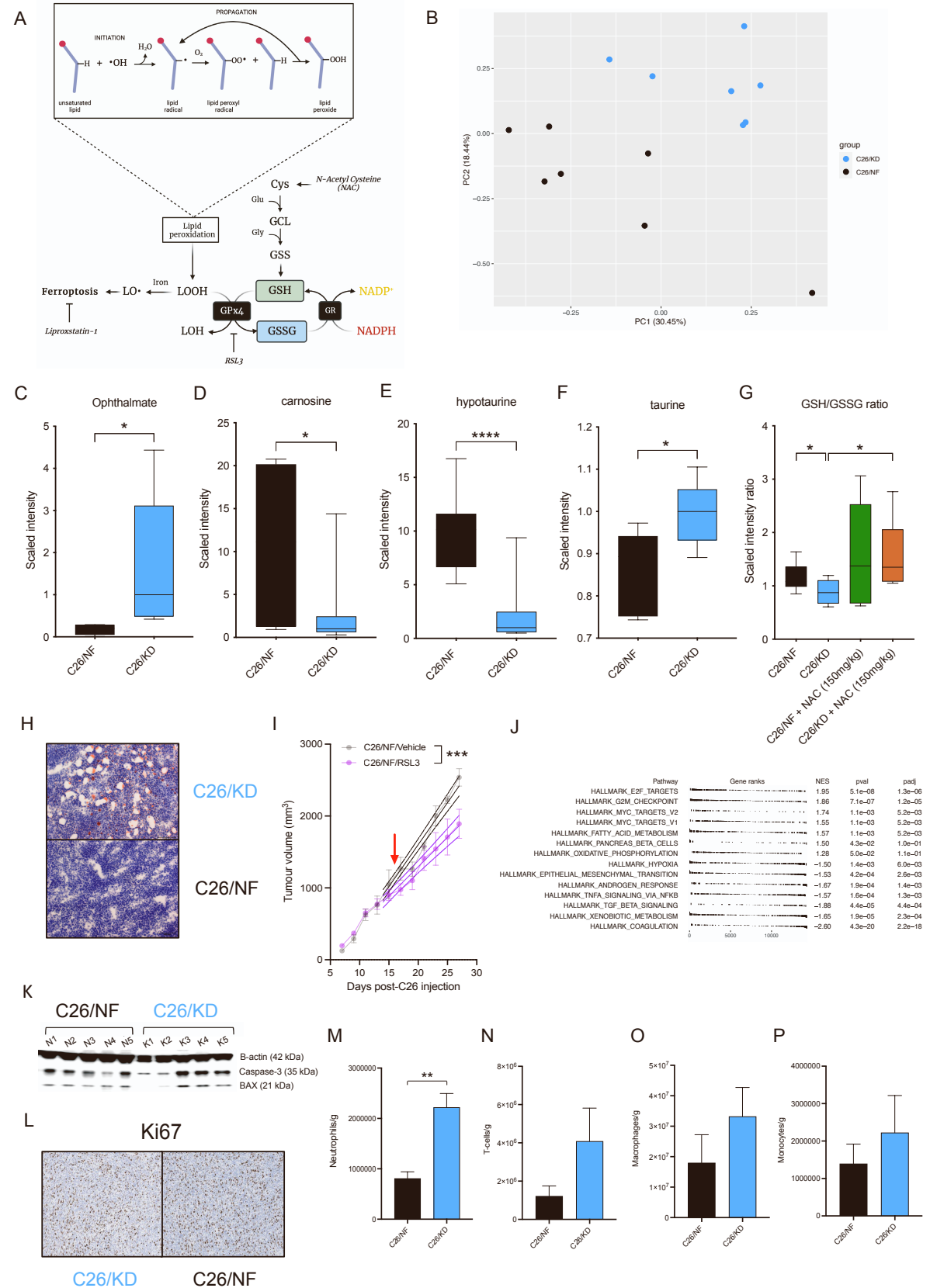


**Figure S2. Intratumoral accumulation of lipids and saturation of the GSH system causes ferroptotic cell death, related to Figure 2.** (A) Schematic representation of the GSH pathway for detoxification of LPPs (Created with BioRender.com). (B) PCA of untargeted metabolomics in the tumors from C26 mice fed KD or NF (n=7). (C-F) Quantification of ophthalmate (C), carnosine (D), hypotauri©(E) and taurine (F) metabolites by UPLC-MS/MS in the tumor of C26 mice fed KD or NF (n=7). (G) Quantification by UPLC-MS/MS of GSH/GSSG ratio in the tumor of C26 mice fed KD or NF, untreated or treated with NAC (n=5-7). (H) Oil-Red-O staining of tumors from C26 mice on KD or NF. (I) Longitudinal tumor volume of C26 mice fed NF and treated with RSL3 or vehicle control (n=4-6). (J) GSEA of upregulated and downregulated pathways in tumors from KPC mice fed KD compared to those fed NF (n=5) (K) Western blot of tumor lysates from C26 mice fed KD or NF stained for Caspase-3 and BAX apoptotic markers (n=5). (L) Immunohistochemistry staining of tumors from C26 mice fed KD or NF with the proliferation marker Ki67. (M-P) Quantification by flow cytometry of neutrophils (M), T-cells (N), macrophages (O) and monocytes (P), in the tumor of C26 mice fed KD or NF (n=3-4).

Statistical analysis in (B and J) is described in Methods. Statistical differences in (C-F, M-P) were examined using an unpaired two-tailed Student's t-test with Welch's correction. One-way ANOVA with Tukey's correction for post hoc testing was used in (G). Simple linear regression model was applied to (I). \* p-value < 0.05, \*\* p-value < 0.01, \*\*\*\* p-value < 0.0001.

**Figure S3**

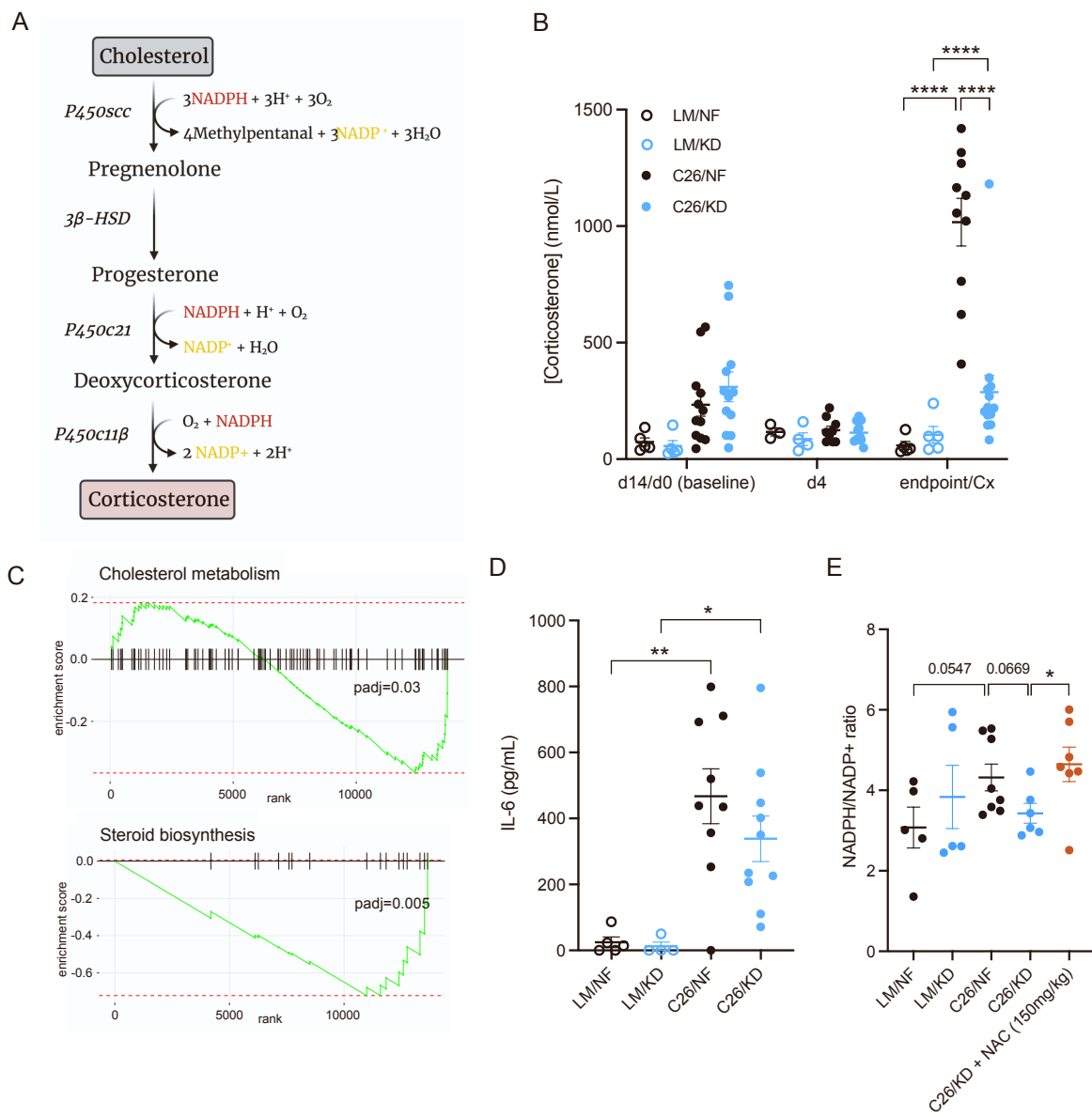


**Figure S3. Biochemical deficiency in the corticosterone synthesis pathway in the adrenal cortex of tumor-bearing mice fed ketogenic diet, related to Figure 3.** (A) Murine synthetic pathway of corticosterone in the cortex of the adrenal glands. (B) Corticosterone levels at baseline (prior to diet change), 4 days after the start of the experiment, and at endpoint (cachexia) in C26 and LM mice fed KD or NF (n=5 LM, n=10-14 C26). (C) GSEA pathway analysis of cholesterol homeostasis and steroid biosynthesis in KD-fed KPC mice compared to NF-fed KPC (n=5). (D) Plasma concentration of the pro-inflammatory cytokine IL-6 in C26 and LM mice on NF or KD diets at endpoint (n=5 LM, n=9-

10 C26). (E) NADPH/NADP<sup>+</sup> ratios in cachectic C26 and LM on NF or KD diets, and C26 mice fed KD and treated with NAC (n=5-8).

One-way ANOVA with Tukey's correction for post hoc testing was used in (B, D, E). Statistical analysis in (C) is described in Methods. \* p-value < 0.05, \*\* p-value < 0.01, \*\*\* p-value < 0.001, \*\*\*\* p-value < 0.0001.

**Figure S4**

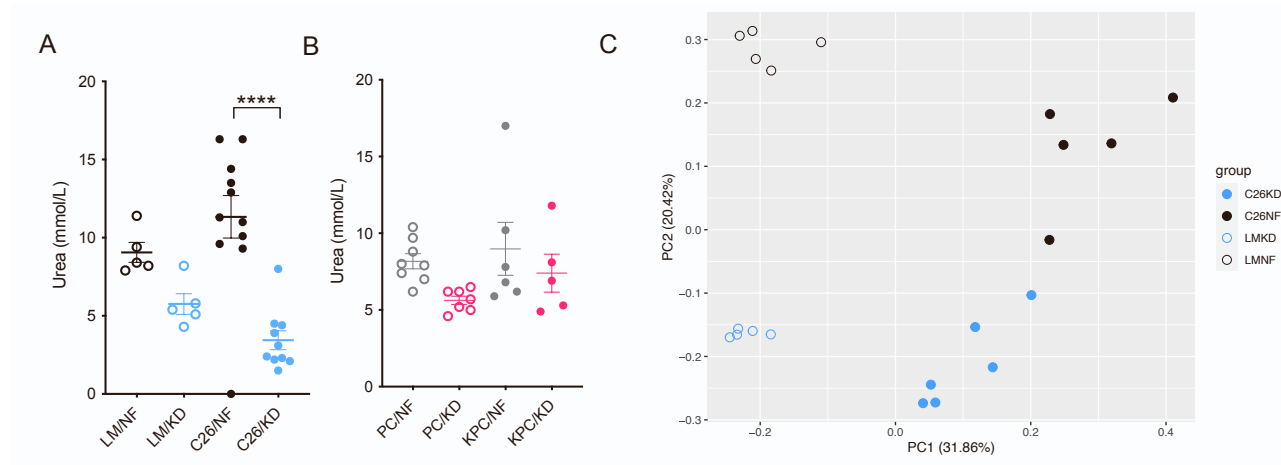


**Figure S4. Extended metabolic profiling of cachectic C26 and KPC mice, related to Figure 5.** (A-B) Plasma urea levels in cachectic C26 and LM mice (n=5 LM, n=10-11 C26) (A), and cachectic KPC and PC mice (n=5-8) (B) fed either KD or NF diet. (C) PCA of hepatic metabolomics in C26 and LM mice fed with KD or NF (n=5-6).

One-way ANOVA with Tukey's correction for post hoc testing was used in (A-B). Statistical analysis in (C) is described in Methods. \* p-value < 0.05, \*\* p-value < 0.01, \*\*\* p-value < 0.0001.

**Figure S5**

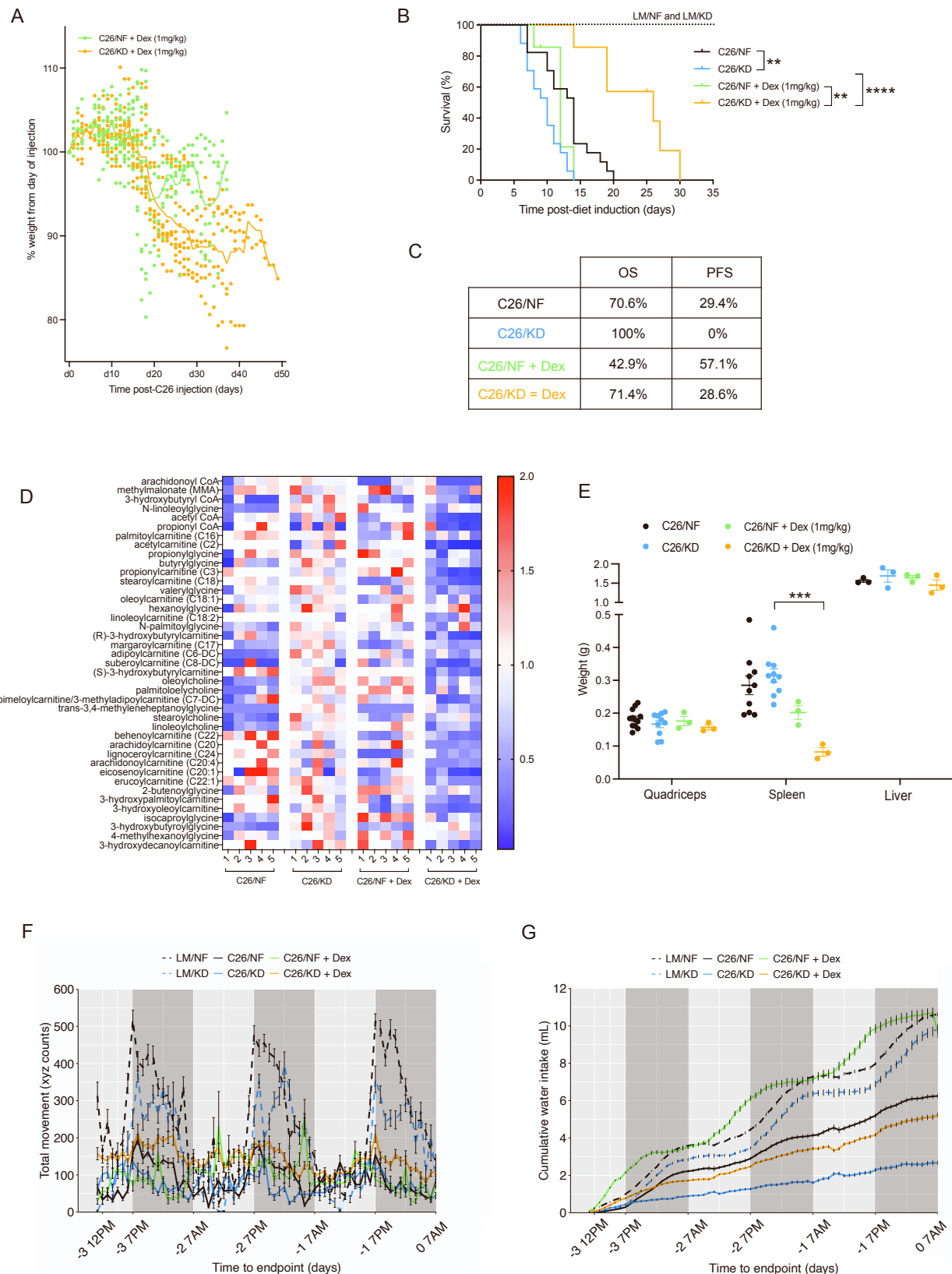


**Figure S5. Extended data on the systemic effects of Dexamethasone treatment, related to Figure 6.** (A) Weight trajectories of C26 mice treated with Dexamethasone and fed with either KD or NF. (B) Survival of LM, and C26 mice treated or untreated with Dexamethasone, fed with KD or NF (n=7 LM, n=17-18 C26, n=7 C26 + Dex). (C) Percentage of mice in each group that were sacrificed because of cachexia (OS) or tumor size (PFS) endpoints. (D) Quantification by UPLC-MS/MS of metabolites involved in fatty acid metabolism in the liver of C26 mice on either KD or NF diets, untreated or treated with Dexamethasone (n=5). (E) Organ weights of C26 mice untreated or treated with Dexamethasone after 4 days of treatment (n=10-12 C26, n=3 C26 + Dex). (F-G) Total movement (F) and cumulative water intake (G) during the last 4 days before endpoint in LM and C26 mice, untreated or treated with Dexamethasone, fed KD or NF (n=7).

Survival: OS + PFS. Kaplan–Meier curves in (B-C) were statistically analyzed by using the log-rank (Mantel–Cox) test. One-way ANOVA with Tukey’s correction for post hoc testing was used in (E). Analysis in (D, F-G) is described in Methods. \* p-value < 0.05, \*\* p-value < 0.01, \*\*\* p-value < 0.001, \*\*\*\* p-value < 0.0001.